Contents lists available at ScienceDirect

Osteoarthritis and Cartilage Open

Patterns of variation among baseline femoral and tibial cartilage thickness and clinical features: Data from the osteoarthritis initiative

Thomas H. Keefe [a], Mary Catherine Minnig [b,c], Liubov Arbeeva [b], Marc Niethammer [d], Zhenlin Xu [d], Zhengyang Shen [d], Boqi Chen [d], Daniel B. Nissman [e], Yvonne M. Golightly [b,c,f], J.S. Marron [a], Amanda E. Nelson [b,c,*]

[a] Statistics and Operations Research, University of North Carolina at Chapel Hill College of Arts and Sciences, Chapel Hill, North Carolina, USA
[b] Thurston Arthritis Research Center, University of North Carolina at Chapel Hill, Chapel Hill, North Carolina, USA
[c] Department of Epidemiology, University of North Carolina at Chapel Hill Gillings School of Global Public Health, Chapel Hill, North Carolina, USA
[d] Department of Computer Science, University of North Carolina at Chapel Hill College of Arts and Sciences, Chapel Hill, North Carolina, USA
[e] Department of Radiology, University of North Carolina at Chapel Hill School of Medicine, Chapel Hill, North Carolina, USA
[f] College of Allied Health Professions, University of Nebraska Medical Center, Omaha, NE 68198, USA

ARTICLE INFO

ABSTRACT

Objective: To employ novel methodologies to identify phenotypes in knee OA based on variation among three baseline data blocks: 1) femoral cartilage thickness, 2) tibial cartilage thickness, and 3) participant characteristics and clinical features.

Methods: Baseline data were from 3321 Osteoarthritis Initiative (OAI) participants with available cartilage thickness maps (6265 knees) and 77 clinical features. Cartilage maps were obtained from 3D DESS MR images using a deep-learning based segmentation approach and an atlas-based analysis developed by our group. Angle-based Joint and Individual Variation Explained (AJIVE) was used to capture and quantify variation, both *shared* among multiple data blocks and *individual* to each block, and to determine statistical significance.

Results: Three major modes of variation were shared across the three data blocks. Mode 1 reflected overall thicker cartilage among men, those with higher education, and greater knee forces; Mode 2 showed associations between worsening Kellgren-Lawrence Grade, medial cartilage thinning, and worsening symptoms; and Mode 3 contrasted lateral and medial-predominant cartilage loss associated with BMI and malalignment. Each data block also demonstrated individual, independent modes of variation consistent with the known discordance between symptoms and structure in knee OA and reflecting the importance of features such as physical function, symptoms, and comorbid conditions independent of structural damage.

Conclusions: This exploratory analysis, combining the rich OAI dataset with novel methods for determining and visualizing cartilage thickness, reinforces known associations in knee OA while providing insights into the potential for data integration in knee OA phenotyping.

Osteoarthritis (OA) has debilitating consequences in terms of pain, physical function, and quality of life for those suffering from the disease. It has been estimated that roughly 13% of Americans—or nearly 31 million individuals—are affected by OA [1]. OA is a progressive disease associated with a gradual loss of cartilage and the degeneration of bone often resulting in joint failure [1,2]. The knee joint is the most common location for OA. Roughly 20% of knee OA cases develop into an accelerated form of the disease, which is more painful and physically limiting, within just four years of initial disease detection [3,4]. In the United States, roughly 700,000 patients annually undergo total knee replacement (TKR) brought on by end-stage knee OA. TKR carries the typical physical risks of surgery, is costly, and has a 10-year revision rate above 6% [5].

There is a growing literature supporting the heterogeneity of the OA disease process. Some studies have delineated OA into different phenotypic groupings characterized by a combination of environmental and

genetic factors [6,7]. This heterogeneity may contribute to the difficulties in identifying appropriate therapeutic strategies for each OA patient [8]. Understanding OA heterogeneity is key to improving clinical decisions in terms of prevention, treatment, and overall disease prognosis [8]. Although OA has often been assessed using conventional radiography methods, magnetic resonance imaging (MRI), offers advantages to visualizing the structural pathology of OA and allows for quantitative measurements of the status of cartilage and bone, which may better characterize the structural heterogeneity in OA.

Recent studies in this area have made use of knee cartilage thickness maps created from MRI to better understand the heterogeneity of the OA disease process. Using anatomically standardized femoral and tibial cartilage thickness maps, a study by Favre et al. was able to determine patterns of cartilage thickness across stages and severity of OA [9]. This group also explored a new computational anatomy technique to improve knee map standardization across time points and individuals [10]. These studies provide a basis for the comparison of knee cartilage thickness maps across individuals; however, previous work has not attempted to integrate multiple knee compartment maps with sociodemographic and participant characteristics—an important step in furthering our understanding of OA heterogeneity [11].

To further the existing work and address some of these gaps, we employed novel methodologies to explore potential phenotypic groups based on statistically shared and individual variation among three data blocks of interest: 1) femoral cartilage thickness, 2) tibial cartilage thickness, and 3) participant characteristics. These methods leverage baseline data collected from the Osteoarthritis Initiative (OAI) database and two methodologies developed by our group: a novel MRI segmentation, registration, and atlas-based analysis process [12]; and Angle-based Joint and Individual Variation Explained (AJIVE) [13] methodology.

1. Methods

Our process had three steps: (1.1) preprocessing the baseline clinical data from the OAI, (1.2) preprocessing the cartilage thickness maps, and (1.3) conducting an AJIVE analysis using the output of (1.1) and (1.2). Before conducting the AJIVE analysis, we split the prepared dataset into two equally sized partitions for internal validation purposes.

1.1. Preprocessing of baseline clinical data

Data used in this study were collected from the OAI, a longitudinal, prospective, observational, multi-center study that is currently in its 14th year of follow-up [14]. This project utilized selected data from the OAI baseline (i.e., *AllClinical00*) and *Enrollees* datasets measured on 4796 individuals with or at risk for knee OA (9592 knees). We selected 72 knee-level and 76 person-level variables (total of 148 variables). These included demographic variables, income, family history, employment and health-care access, knee and/or hip injury, surgery, fractures, falls, knee and hip symptoms including at rest and with activity, frequent knee pain, knee exam findings, isometric strength, physical performance tests, and medical history including comorbidity and medications.

Our preprocessing of this dataset comprised the following. Standardization of numeric variables was performed with a shifted log transformation to reduce skewness [15]. When needed, new variables, including medication and knee surgery history were created (for example, per the OAI protocol, if the response to P01KSURGR was 0, then none of the follow-up questions [i.e., P01ARTR, P01ARTRINJ, P01LRR, P01MENR, P01MENRINJ] were asked, and were therefore missing; these variables were set to "0" for participants with P01KSURGR = 0). Binary "dummy" variables were created from nominal variables such as race. The data were converted from person-level to knee-level format (72 variables with left/right information were collapsed into 36, with one variable created to identify left/right side). Variables pertaining to the left and right *hips* were recoded as ipsilateral and contralateral with

respect to each *knee*. Certain variables were excluded for being too granular, or exhibiting no variation, or being otherwise uninformative. Our processing yielded 77 variables as input to AJIVE (Table 1). We then excluded any knee that had missing data on any of the 77 measures (leaving 6317 knees), and any knee that did not have baseline femoral and tibial cartilage maps (leaving 6266 knees). Finally, one knee was excluded for being an extreme outlier, leaving our analytic set of n = 6265 knees.

1.2. Preprocessing of baseline cartilage maps

We used the baseline cartilage maps produced by Niethammer et al. [12] (Fig. 1). Femoral and tibial cartilage was segmented from the OAI 3D DESS MR images using a 3D U-Net (for this analysis at https://github.com/uncbiag/OAI_analysis; with additional updates at https://github.com/uncbiag/OAI_analysis_2). Thickness was measured to the closest point of the opposing surface of the segmented cartilages and transferred to an atlas space via deep-learning-based deformable image registration, resulting in local spatial correspondences between all patients and all timepoints [12]. This 3D segmentation network was previously evaluated using knee MRIs from the OAI with available manual segmentations of femoral and tibial cartilage [16]. These data consisted of 176 images from 88 patients (two longitudinal scans per patient). The dataset was split by patient into training (60 patients, 120 images), validation (8 patients; 6 images), and test (20 patients; 40 images) sets. We achieved a Dice overlap score of 0.90 (standard deviation 0.02) for femoral cartilage and 0.89 (standard deviation 0.03) for tibial cartilage respectively [16]. To facilitate analysis, the cartilage volumes in the 3D atlas space were unrolled/projected to 2D, 310 by 310 pixel arrays in the axial plane, with the value at each pixel representing the cartilage thickness in mm (Fig. 1A). Femoral cartilage was unrolled cylindrically, and tibial cartilage was projected orthographically. To eliminate symmetry, right knees were reflected across the sagittal plane to spatially match the left knees.

For input to AJIVE, we processed the cartilage map dataset described above in two steps. First, a small number of pixel locations had null values and were excluded for all 6265 knees (Fig. 1B). Second, we flattened the 2D arrays to 1D vectors, omitting null pixel locations. The resulting femoral vectors contained 57,260 pixels each, and the tibial vectors 56,340 pixels each. While cartilage maps had been produced for all timepoints from baseline to 96 months, this analysis used only the baseline maps and features.

1.3. Angle-based Joint and Individual Variation Explained (AJIVE)

The data in this analysis comprise three *data blocks*: (i) femoral cartilage maps (ii) tibial cartilage maps, and (iii) participant/clinical characteristics from the OAI. Data blocks refer to sets of measurements taken on the same set of observations that are expected to have differing patterns of variation [17]. For example, we should expect there to be variation visible in the participant characteristics block that is not reflected in the two cartilage blocks. AJIVE is a method developed by our group to understand the modes of variation expressed across multiple data blocks [13,18]. AJIVE captures (1) shared (or "joint") structure among all three data blocks and (2) structure individual to each data block. The modes of variation are visualized using loadings plots, which show the contribution of each cartilage pixel and of each clinical variable to a given mode of variation. A set of scores is generated for each knee that represents the extent to which each knee expresses these modes. These scores are visualized using scatterplots, where each knee is one point in the plot, with its coordinates in the plot denoting its scale-free scores and therefore relative magnitudes for the different modes. For richer analysis, the points were colored by variables of interest, such as the baseline Kellgren-Lawrence Grade (KLG, from 0 to 4).

In addition to shared modes, AJIVE also finds individual modes of variation, which refer to variation in one data block that does not correspond with variation in the other data blocks. AJIVE returns these

Table 1
OAI variables and status in the analysis.

Variable Description	OAI variable name
Person-level variables-included	
Female sex	P02SEX
Hispanic or Latino, self-reported	P02HISP
White or Caucasian race	P02RACE
Black or African American race	P02RACE
Asian race	P02RACE
SF-12 Physical Health Summary	V00HSPSS
SF-12 Mental Health Summary	V00HSMSS
Marital status: Widowed	V00MARITST
Marital status: Divorced	V00MARITST
Marital status: Separated	V00MARITST
Marital status: Never married	V00MARITST
Currently employed	V00CUREMP
Yearly income >50 K (calc)	V00INCOME2
Have medical insurance	V00MEDINS
Age (calc, used for study eligibility)	V00AGE
Highest grade or year of school completed (calc)	V00EDCV
How many alcoholic drinks in typical week, past 12 months	V00DRNKAMT
Comorbidity Score	V00COMORB
Center for Epidemiologic Studies Depression Scale (CES-D) Score (calc)	V00CESD
Physical Activity Scale for the Elderly	V00PASE
Blood pressure: systolic (mm Hg)	V00BPSYS
Blood pressure: diastolic (mm Hg)	V00BPDIAS
Body mass index (calc)	P01BMI
Fallen and landed on floor or ground, past 12 months	V00FALL
Smoked at least 100 cigarettes (5 packs) in entire life	V00SMOKE
In the past, did drink more beer, wine or liquor than now	V00DRKMORE
Total number of medications recorded	V00RX30NUM, V00RX30
Used analgesic in last 30 days	V00RXANALG
Used narcotic analgesic in last 30 days	V00RXNARC
Injected corticosteroid in last 30 days	V00RXISTRD
Used COX-II inhibitor in last 30 days	V00RXCOX2
Used NSAID in last 30 days	V00RXNSAID
Ever had hip replacement surgery where all or part of joint was replaced	P01HRS
Doctor ever said participant broke or fractured bone after age 45	V00BONEFX
Doctor ever said participant fractured spine or vertebrae	V00SPNFX
Repeated chair stand: pace in stands/sec (calc)	V00CSPACE
Able to complete 5 repeated chair stands	V00CS5
20-m walk: pace (m/sec) (calc)	V0020MPACE
400-m walk	V00400MTIM
Family history of TKR	P02FAMHXKR
Presence of hip pain (right), aching or stiffness: any, past 12 months (includes pain in groin and in front and sides of upper thigh)	P01HPNR12_1: Yes
Presence hip pain (left), aching or stiffness: any, past 12 months (includes pain in groin and in front and sides of upper thigh)	P01HPNL12_1: Yes
Presence of back pain (any), past 30 days	P01BP30
Presence of right hip pain, aching or stiffness: more than half the days of a month, past 12 months (calc)	P01HPR12CV
Presence of left hip pain, aching or stiffness: more than half the days of a month, past 12 months (calc)	P01HPL12CV
Person-level variables-excluded	
Single chair stand	V00CSTSGL
Left hip pain, aching or stiffness location: groin/inside leg near hip	P01HPNLIL
Right hip pain, aching or stiffness location: groin/inside leg near hip	P01HPNRIL
Bring in or identify all prescription	V00RX30
Valdecoxib use indicator	V00RXVLCXB
Calcitonin use indicator	V00RXCLCTN
Bisphosphonate use indicator	V00RXBISPH
Injected hyaluronic acid use indicator	V00RXIHYAL
Rofecoxib use indicator	V00RXRFCXB

Table 1 (*continued*)

Variable Description	OAI variable name
Chondroitin sulfate use indicator	V00RXCHOND
Other analgesic use indicator	V00RXOTHAN
Glucosamine use indicator	V00RXGLCSM
Acetaminophen use indicator	V00RXACTM
Aspirin use indicator	V00RXASPRN
Nitrate use indicator	V00RXNTRAT
Raloxifene use indicator	V00RXRALOX
Vitamin D use indicator	V00RXVIT_D
Oral corticosteroid use indicator	V00RXOSTRD
Celecoxib use indicator	V00RXCLCXB
Teriparatide use indicator	V00RXTPRTD
Salicylate use indicator	V00RXSALIC
Fluoride use indicator	V00RXFLUOR
Methylsulfonylmethane use indicator	V00RXMSM
S-adenosylmethionine use indicator	V00RXSAME
Current employment	V00CEMPLOY
Subcohort assignment (calc)	V00COHORT
Knee level variables-included	
Ever injured badly enough to limit ability to walk for at least two days	P01INJL, P01INJR
Ever have knee surgery or arthroscopy	P01KSURGL, P01KSURGR
Ever have knee arthroscopy (where they put a scope in knee)	P01ARTL, P01ARTR, P01KSURGL, P01KSURGR
Ever have meniscectomy (where they repaired or cut away torn meniscus or cartilage)	P01MENL, P01MENR, P01KSURGL, P01KSURGR
Ever have ligament repair surgery	P01LRL, P01LRR, P01KSURGL, P01KSURGR
WOMAC Pain Score (calc)	V00WOMKPL, V00WOMKPR
KOOS Pain Score	V00KOOSKPL, V00KOOSKPR
WOMAC Stiffness Score (calc)	V00WOMSTFL, V00WOMSTFR
KOOS Symptoms Score	V00KOOSYML, V00KOOSYM
WOMAC Disability Score (calc)	V00WOMADLL, V00WOMADLR
Isometric strength: leg weight (N)	V00LWGTL, V00LWGTR
Isometric strength: knee extension, severity of pain (calc)	V00LEXP1CV, V00REXP1CV
Isometric strength: knee flexion, severity of pain (calc)	V00LFXP1CV, V00RFXP1CV
knee exam: flexion contracture/hyperextension, degrees (contracture positive) (calc)	V00LKFHDEG, V00RKFHDEG
knee exam: alignment, degrees (valgus negative) (calc)	V00LKALNMT, V00RKALNMT
Flexion MAX Force	V00rfmaxf, V00lfmaxf
Flexion Speed of Force Relaxation	V00lfSFR, V00rfSFR
Extension Speed of Force Production	V00leSFP, V00reSFP
Extension Speed of Force Relaxation	V00leSFR, V00reSFR
Flexion Speed of Force Production	V00lfSFP, V00rfSFP
Knee pain, aching or stiffness: any, past 12 months	P01KPNL12, P01KPNR12
Knee exam: presence of patellar quadriceps tendinitis, pain/tenderness at any four sites	V00LKPATPN, V00RKPATPN
Knee exam: effusion, bulge sign positive	V00LKEFFB, V00RKEFFB
Knee exam: effusion, patellar tap positive	V00LKEFFPT, V00RKEFFPT
Knee is to tender to examine	V00LKEFFPT, V00RKEFFPT
presence of knee flexion pain/tenderness on knee exam	V00RKRFXPN, V00LKRFXPN
Presence of lateral tibiofemoral pain/tenderness on knee exam	V00LKLTTPN, V00RKLTTPN
Presence of medial tibiofemoral pain/tenderness on knee exam	V00LKMTTPN, V00RKMTTPN
Presence of anserine bursa, pain/tenderness on exam	V00LKABPN, V00RKABPN
Knee exam: patello-femoral crepitus present on exam	V00LKPFCRE, V00RKPFCRE
Knee exam: patellar grind, painful or tender behind kneecap	V00LKPGDPN, V00RKPGDPN
BL knee symptom status	P01LKSX, P01RKSX
Knee level variables-excluded	
At least one meniscectomy to repair an injury	P01MENLINJ, P01MENRINJ, P01KSURGL, P01KSURGR
At least one arthroscopy to repair knee injury	P01ARTLINJ, P01ARTRINJ, P01KSURGL, P01KSURGR
Knee exam: alignment varus or valgus (calc)	V00LKDEFCV, V00RKDEFCV
WOMAC Total Score (calc)	V00WOMTSL, V00WOMTSR
Summary incident TF ROA KL≥2 (calc)	V99ELXIOA, V99ERXIOA
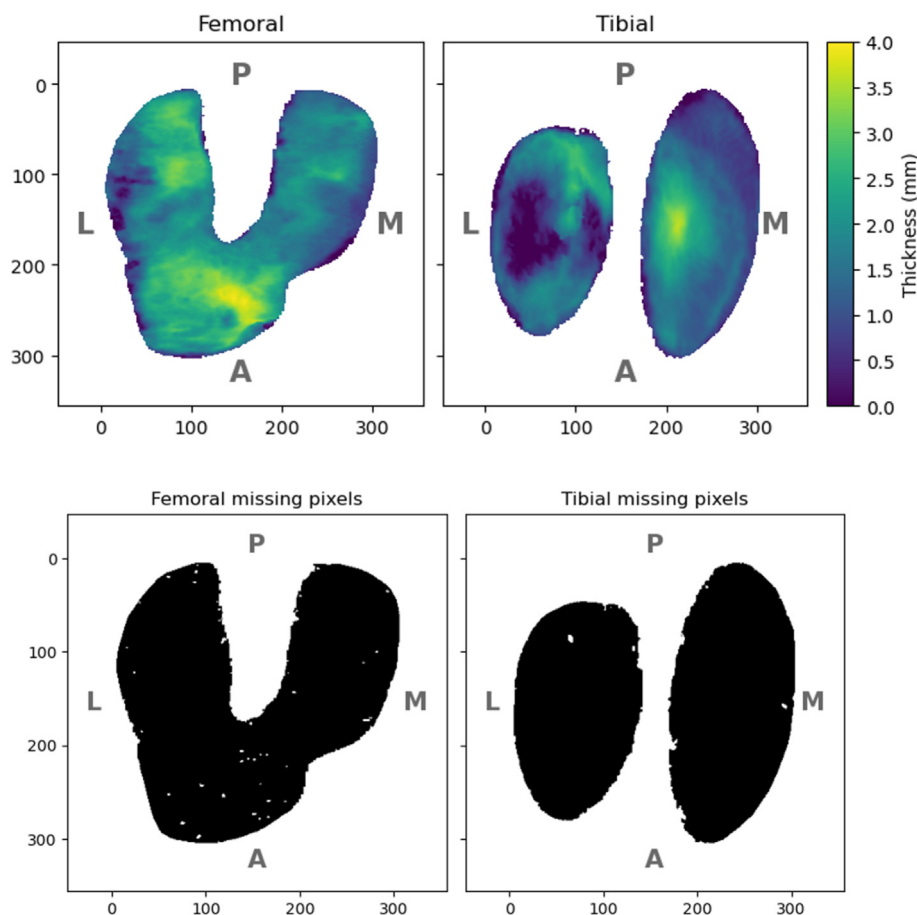
Fig. 1. 2D cartilage maps. 1A) femoral and tibial 2D thickness pixel arrays (310 × 310) colored from dark blue (thinnest) to yellow (thickest) areas. Medial, lateral, anterior, and posterior aspects are annotated (M, L, A, and P, respectively). 1B) Pixel locations with null values for any knee (white areas) were excluded for all 6390 knees. (For interpretation of the references to colour in this figure legend, the reader is referred to the Web version of this article.)

individual modes in order of variance explained, similar to principal component analysis. The software implementation of AJIVE that we used is available at: https://doi.org/10.5281/zenodo.4091752.

Statistical significance of the number of shared modes and of the contribution of each variable to those modes (loadings) were assessed. Statistical significance of the loadings (i.e., whether a particular cartilage pixel or OAI feature has a nonzero influence on a mode of variation) was assessed using a modification of the jackstraw method [19] for principal component analysis. We show only the loadings that are statistically distinguishable from zero (with a targeted false-discovery rate of 1% [20]). For internal validation, we split our baseline dataset at random into two equally sized partitions (at the person-level) and repeated the analysis on each. Partition 1 contains 3127 knees from 1661 individuals, and Partition 2 contains 3138 knees from 1660 individuals (software workflow available at: https://github.com/thomaskeefe/baseline cartilage).

2. Results

2.1. Directions of shared variation

The top three directions of shared variation (i.e., modes) between these three data blocks were consistent in the two partitions (providing internal validation) and are shown in Fig. 2. **Shared direction 1** (Fig. 2, column 1; 2.1) reflected features associated with thicker baseline cartilage overall and was bimodal based on sex (**2.1.A**). Knees with thicker (red) femoral (**2.1.B**) and tibial (**2.1.C**) cartilage were characterized by higher knee flexion force and speed of force production/relaxation, male

sex, higher education, and faster 400 m walk time (**2.1.D**). Particularly for Shared direction 2 (Fig. 2.2), there was a clear association between worsening KLG (2.2.A-B) and cartilage thinning (blue) in the medial femur (2.2.C) and most of the tibia (2.2.D). Features associated with variation in this direction included greater knee flexion contracture, more symptoms (lower KOOS and higher WOMAC), poorer physical health, older age, and higher BMI (2.2.D). Shared direction 3 (Fig. 2.3) represented a spectrum between lateral-predominant thinning and medial predominant thinning (2.3.D-E), where lateral thinning was associated with higher BMI, valgus knee alignment, Black race, slower walking speeds, and more chair stands per second (2.3.F), while medial thinning was associated with varus alignment, lower BMI, White race, faster walking speed, and fewer chair stands completed.

2.2. Directions of individual variation: clinical variables

In addition to the shared modes, we examined the *individual* modes of variation for each of the variable blocks. For the clinical features, these modes reflected the ways that these features varied <u>independently</u> of femoral and tibial cartilage. Figs. 3 and 4 show the top three (in terms of variance explained) directions of individual variation among the clinical variables. Of note, while the shared modes (Fig. 2) had a strong association with the KLG, none of that relationship remained in the individual modes, as demonstrated by the lack of color gradient by KLG in Fig. 3. This indicates that there was <u>no</u> additional information relevant to KLG in the clinical variables that was not already present in the cartilage maps. In contrast, a clear color gradient was seen if these same individual modes of variation were colored instead by WOMAC pain (Fig. 4). The
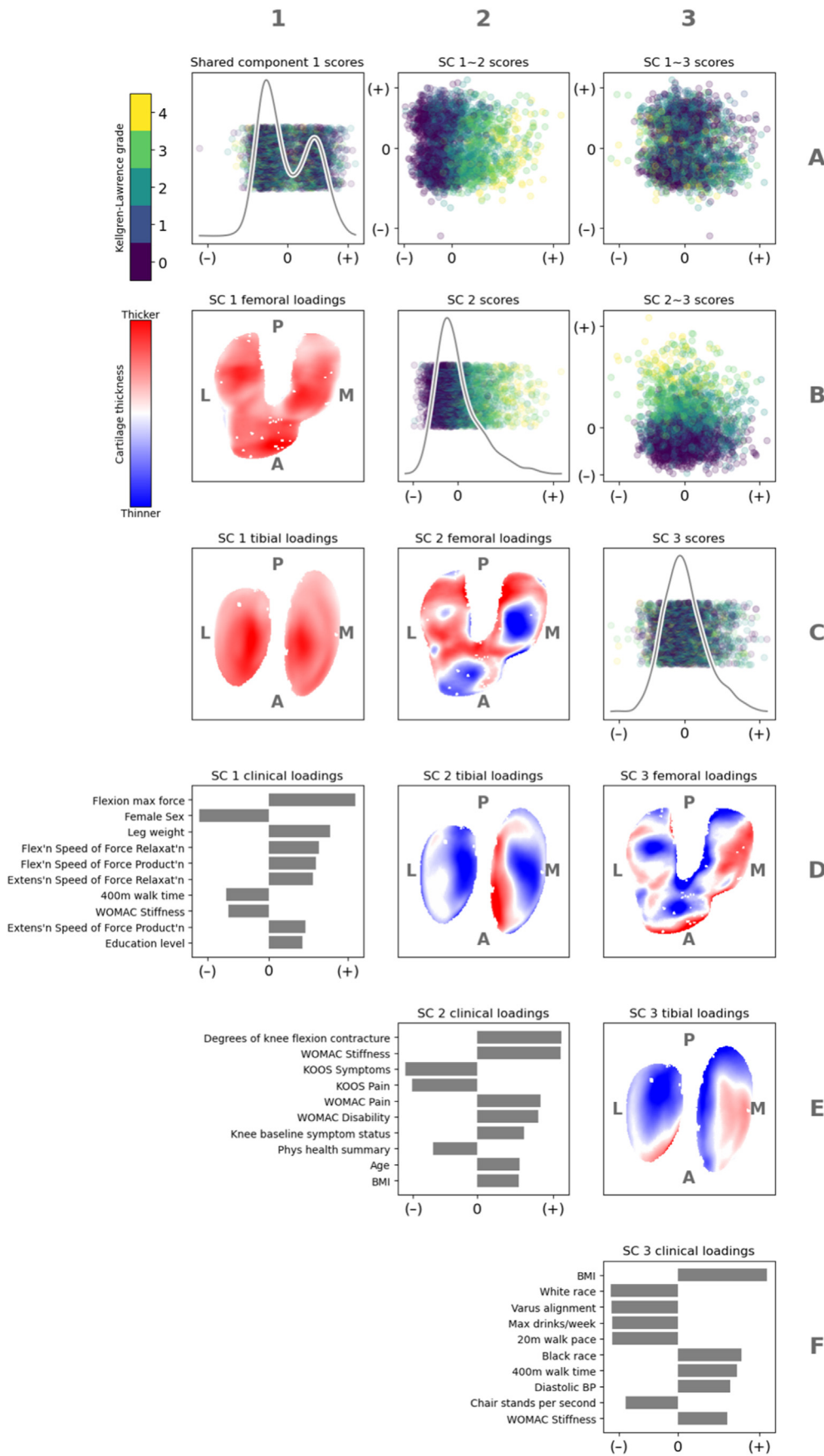
Fig. 2. First 3 directions (columns 1–3) representing shared variation in femoral cartilage thickness, tibial cartilage thickness, and clinical features based on AJIVE analysis using OAI baseline data. The black curves on the diagonal plots indicate the kernel density estimate for the distribution of the scores. Location of each knee in the coordinate system defined by the shared directions are shown in panels 2.1.A, 2.2.A, 2.3.A, 2.2.B, 2.3.B, and 2.3.C, colored by the baseline Kellgren-Lawrence grade (ordinal, 0 = purple to 4 = yellow). Femoral cartilage variation in each direction is shown in 2.1.B, 2.2.C, and 2.3.D; corresponding tibial cartilage variation is shown in 2.1.C, 2.2.D, and 2.3.E; thicker cartilage is red, thinner cartilage is blue. The ten largest magnitude statistically significant feature loadings are represented by the bar plots in 2.1.D, 2.2.E, and 2.3.F (indicating either negative (−) or positive (+) direction of the loading). (For interpretation of the references to colour in this figure legend, the reader is referred to the Web version of this article.)
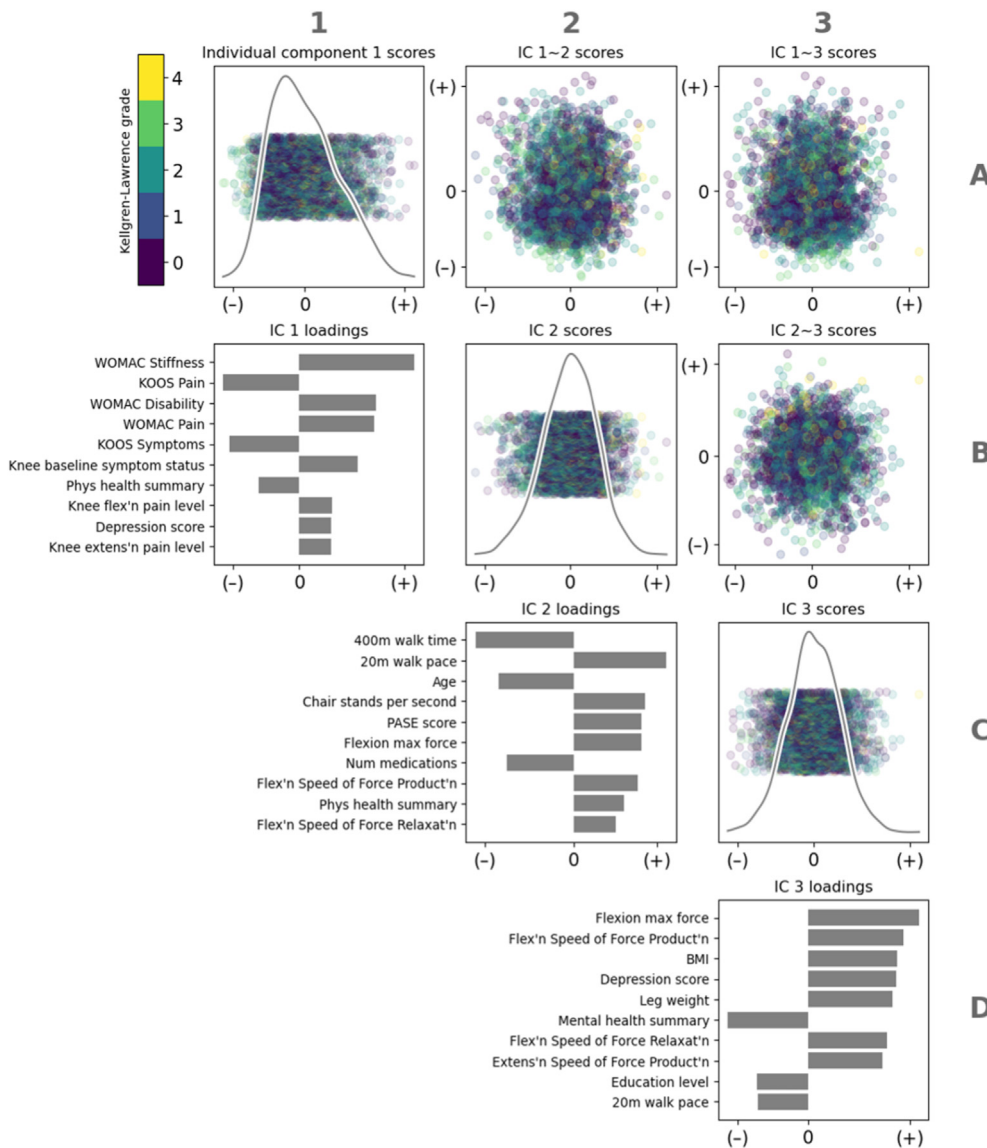
Fig. 3. Top 3 directions (columns 1–3) representing variation in the clinical features that are <u>not</u> related to femoral and tibial cartilage based on AJIVE analysis using OAI baseline data. The color scale in 3.1.A, 3.2.A-B, and 3.3.A-C is by Kellgren-Lawrence grade (as in Fig. 2). The ten largest magnitude statistically significant feature loadings are represented by the bar plots in 3.1.B, 3.2.C, and 3.3.D. (For interpretation of the references to colour in this figure legend, the reader is referred to the Web version of this article.)

smooth color gradient demonstrated variability in self-reported pain that did *not* correspond with variation in the cartilage. The individual directions in Fig. 4 represent the same data, the same loadings, and have the same interpretation as in Fig. 3, just with different coloring.

In both Figs. 3 and 4, individual direction 1 corresponds to variability in knee symptoms. It was characterized by poorer KOOS and WOMAC scores, pain on knee flexion and extension pain, poorer physical health, and higher depression scores. Individual direction 2, in contrast, was not related to symptoms, but rather characterized a spectrum from younger, more active people (faster walking time and chair stand pace, higher PASE and physical health) with fewer medications; to older, less active, more medicated people. Finally, Individual direction 3 represented the general level of forces generated at the knee. Larger force measures were associated with greater BMI, lower educational attainment, and worse depressive symptoms (SF-12 and CES-D).

2.3. Directions of individual variation: femoral and tibial

The femoral and tibial cartilage maps also demonstrated modes of individual variation that were independent of each other <u>and</u> of the clinical variables. The three largest modes of femoral individual variation (Fig. 5) all involved contrasts between the anterior aspect of the femur (interpretable as the area under the patella) and the medial and lateral condyles. Individual direction 1 (5.1) described overall femoral cartilage thickness, with particular emphasis on the anterior femoral surface. Individual direction 2 (5.2) described focal loss of anterior cartilage thickness versus that in the medial and femoral condyles. Individual direction 3 (5.3) suggested an aspect of anterior to posterior tilt and may reflect a component of tricompartmental involvement. Again, these three modes of variation were unrelated to any variation in the tibial and clinical variables.

The three largest modes of individual variation in the tibial maps are shown in Fig. 6. The first individual direction described thickness of the medial versus the lateral tibial cartilage (6.1). The second (6.2) described a contrast between the more lateral aspect portion of the medial tibial cartilage plate and the remainder of the tibial cartilage. The third (6.3) suggested anterior to posterior variation in cartilage thinning over the tibia, independent of the femoral cartilage and clinical features.

3. Discussion

Three major modes of variation were shared across the three data blocks. These directions are interpretable, reflecting known aspects of knee OA, but also provide additional associations by utilizing all the
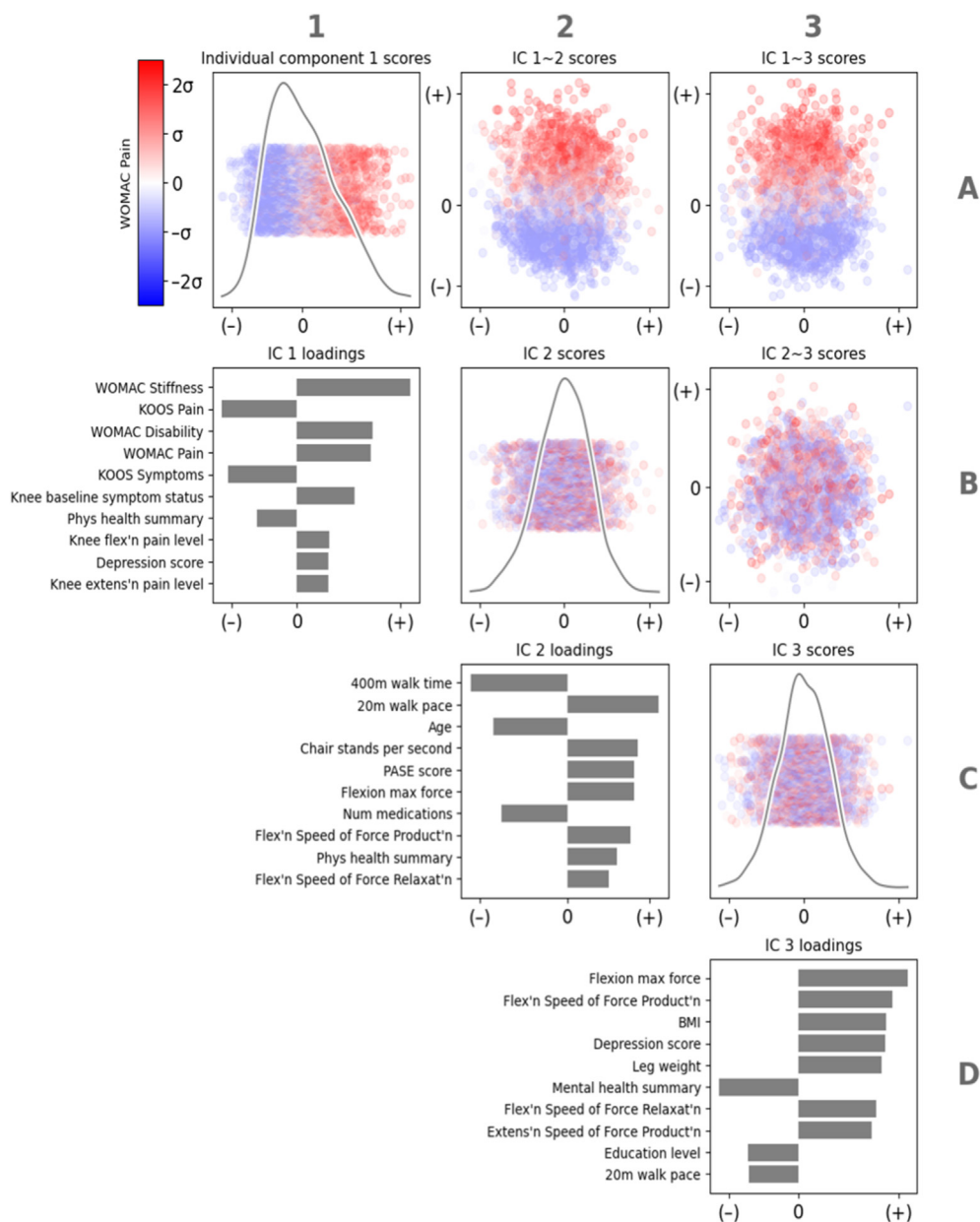
Fig. 4. The same individual modes as in Fig. 3, but now colored by WOMAC Pain (blue = lower WOMAC score or fewer symptoms; red = higher WOMAC score or more symptoms). (For interpretation of the references to colour in this figure legend, the reader is referred to the Web version of this article.)

available data in an advanced analytic method. These shared modes represent features that are associated with clinical features and cartilage loss. In contrast, the individual modes of variation in the clinical features vary independent of cartilage thinning and are not associated with KLG. However, these features, including physical function, symptoms, and comorbidity, are known to affect the prognosis of OA, and are often poorly or incompletely assessed in studies, particularly those focused on structure rather than symptoms. Finally, the femoral and tibial individual modes of variation quantify variation in femoral cartilage that is independent of tibial cartilage and vice versa, as well as independent of the clinical features included in this analysis.

Advanced methodology for analysis of MRI and other medical imaging data is a rapidly growing area in OA [21]. Several groups have proposed deep-learning models based on image data, including morphologic features and T2 relaxation times, to predict outcomes such as radiographic or symptomatic progression or joint replacement in knee OA [21–25]. For example, Lee et al. employed an ensemble deep learning

model of clinical and MR image features to predict 8-year pain trajectories in the OAI, although this model did not provide detailed examination or visualization of other associated features [25]. Similarly, prediction of TKR from MR images incorporated but did not further explore associations with clinical variables such as those utilized in this work [23]. Of particular interest is a recent paper that incorporated not only cartilage thickness (averaged over the femur and tibia rather than by compartment), but also MR-defined bone shape and T2 relaxation times to identify potential biomarkers of chronic pain, but again did not attempt to visualize associations among the different features [26]. This group utilized a spherical transformation (defining MRI features as points on a sphere) which requires establishing a spherical coordinate system and implicitly assumes correspondences for given spherical coordinates [26]. In contrast, our approach [12] makes use of a highly computationally efficient deep registration network which allows spatially transforming a 3D image (and its associated thickness map) to a 3D common atlas image followed by a fixed 2D projection step from 3D to
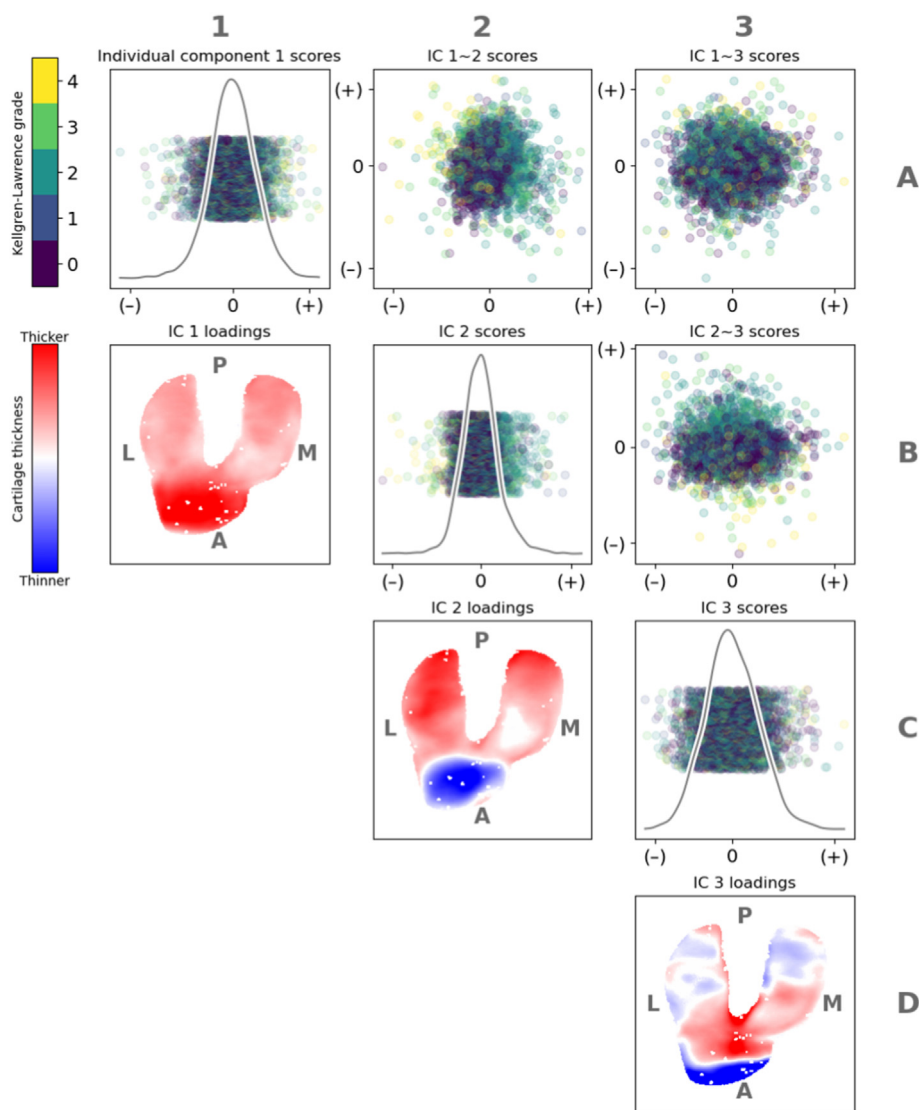
Fig. 5. First 3 directions (columns 1–3) representing individual variation in femoral cartilage thickness <u>not</u> related to the clinical features, based on AJIVE analysis using OAI baseline data.

2D atlas space. Hence, a good spatial correspondence is explicitly constructed.

In addition to this novel registration network, the AJIVE methodology [13] addresses the challenge of associating large sets of disparate data (e.g., MRI features, clinical and sociodemographic features, biochemical markers) on a common set of participants; a paradigm occurring more often as ML and AI techniques are increasingly utilized in OA research.

The shared modes identified here among femoral cartilage, tibial cartilage, and clinical variables are a composite of what has been found over many years in many individual studies of knee OA [2]. Thicker cartilage is seen in men, those generating higher knee forces, with greater education, and faster walk times (shared direction 1). Medial cartilage thinning is seen in those with worse symptom scores, higher BMI, older age, and poorer physical function (shared direction 2), also in line with risk factors for accelerated knee OA in the OAI [27]. Lateral vs medial thinning is seen based on malalignment direction, BMI, race, and physical activity scores (shared direction 3). These findings highlight known differences in OA by sex [21,28] and race [2,29,30] (although the proportion of non-white participants in the OAI is small). Malalignment is known to increase risk and progression of knee OA [2] and has also been proposed as a potential phenotypic subgroup in OA [7,28]. Additionally,

we and others have shown variations in alignment, lateral OA, and valgus thrust by race [31,32] consistent with these findings.

The individual variation in the clinical data block yielded interesting findings that, while unrelated to cartilage thinning, quantify known and hypothesized aspects of clinical knee OA. Firstly, the largest component of individual clinical variation concerns symptomatic variables (Fig. 3.1). This reinforces the fact that variation in knee pain and symptoms is not well-explained by structural features of knee OA (e.g., cartilage loss). Other large modes of variation in the individual space concern physical activity (3.2), and force generation that is unexplained by age and sex (3.3).

The individual modes of cartilage thickness (that vary independently for the femur vs. the tibia vs. the clinical features, Figs. 5 and 6) seem to at least in part describe thickness of the anterior femur, and focal cartilage loss in this area, that may suggest involvement of the patellofemoral joint (PFJ), although we cannot directly assess this as our current maps do not include the patellar cartilage. PFJ involvement in OA is not rare [33], is less frequently studied compared to tibiofemoral involvement [34], and in combination the two likely result in poorer function than either alone [35]. Specific shape changes on MRI at the PFJ have been associated with PFJ OA [36]. In addition to the lack of patellar cartilage
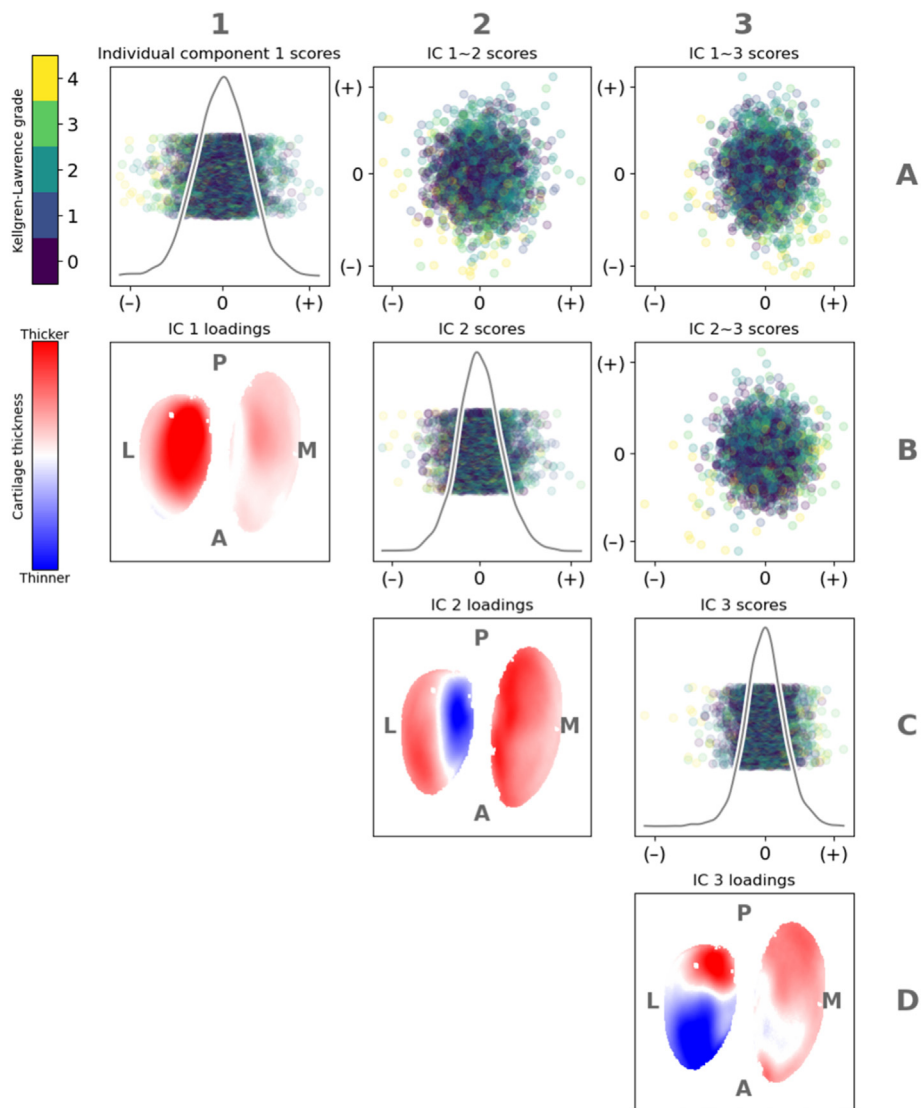
Fig. 6. First 3 directions (columns 1–3) representing individual variation in tibial cartilage thickness <u>not</u> related to the clinical features, based on AJIVE analysis using OAI baseline data.

segmentation, the analysis is limited by the cohort under study, which includes only those with or at risk for knee OA and therefore is not widely generalizable to other groups, and the lack of an available cohort for robust external validation.

Strengths of this work include the large, publicly available OAI dataset, the novel cartilage thickness assessment, and application of AJIVE methodology, including statistical inference and internal validity. Limitations include the lack of a comparable external cohort for fully independent validation, and the lack of novel features available in the OAI dataset. While the current work focuses on baseline features, these methodologies can be applied to longitudinal cartilage maps and clinical features in future work. This initial work demonstrates the utility of these novel tools in various settings and across datasets.

4. Conclusions

This exploratory analysis, combining the rich OAI dataset with novel methods for determining and visualizing cartilage thickness as well as for assessing variation within and among data blocks, reinforces known associations in knee OA while providing insights into the potential for data integration in knee OA phenotyping.

Author contributions

Conception and design: THK, LA, MN, YMG, JSM, AEN.Analysis and interpretation of the data: THK, MCM, LA, MN, ZX, ZS, BC, DBN, YMG, JSM, AEN.Drafting of the article: THK, MCM, LA, AEN.Critical revision of the article for important intellectual content: MN, ZX, ZS, BC, DBN, YMG, JSM.Statistical expertise: THK, LA, JSM.Obtaining of funding: MN, YMG, JSM, AEN.Final approval of the article to be submitted: all.

Funding

by the NIH, a branch of the Department of Health and Human Services and conducted by the OAI Study Investigators. Funding partners include Merck Research Laboratories, Novartis Pharmaceuticals Corp., GlaxoSmithKline, and Pfizer Inc. The funders had no role in study design, data collection and analysis, decision to publish, or preparation of the manuscript.

Data reporting

All OAI data used in this paper are publicly available. Data and/or research tools used in the preparation of this manuscript were obtained and analyzed from the controlled access datasets distributed from the Osteoarthritis Initiative (OAI), a data repository housed within the NIMH Data Archive (NDA). Dataset identifier(s): NIMH Data Archive Collection ID: 2343. Analysis pipeline available at: https://github.com/thomaskeefe/baselinecartilage.

Declaration of competing interest

Drs. Nelson and Golightly have received grant funding unrelated to this work from the Centers for Disease Control and Prevention and NIH/NIAMS and are Associate Editors of *Osteoarthritis and Cartilage*. Dr. Nelson is a Board Member of the Osteoarthritis Research Society International (OARSI).

References

[1] X. Zhao, D. Shah, K. Gandhi, W. Wei, N. Dwibedi, L. Webster, et al., Clinical, humanistic, and economic burden of osteoarthritis among noninstitutionalized adults in the United States, Osteoarthritis Cartilage 27 (2019) 1618–1626, https://doi.org/10.1016/j.joca.2019.07.002.

[2] J.N. Katz, K.R. Arant, R.F. Loeser, Diagnosis and treatment of hip and knee osteoarthritis: a review, JAMA 325 (2021) 568–578, https://doi.org/10.1001/jama.2020.22171.

[3] M.S. Harkey, J.E. Davis, L.L. Price, R.J. Ward, J.W. MacKay, C.B. Eaton, et al., Composite quantitative knee structure metrics predict the development of accelerated knee osteoarthritis: data from the osteoarthritis initiative, BMC Muscoskel. Disord. 21 (2020) 299, https://doi.org/10.1186/s12891-020-03338-7.

[4] L.L. Price, M.S. Harkey, R.J. Ward, J.W. MacKay, M. Zhang, P. et al., Role of magnetic resonance imaging in classifying individuals who will develop accelerated radiographic knee osteoarthritis, J. Orthop. Res. 37 (2019) 2420–2428, https://doi.org/10.1002/jor.24413.

[5] U. Heilmeier, J.M. Wamba, G.B. Joseph, K. Darakananda, J. Callan, J. Neumann, et al., Baseline knee joint effusion and medial femoral bone marrow edema, in addition to MRI-based T2 relaxation time and texture measurements of knee cartilage, can help predict incident total knee arthroplasty 4-7 years later: data from the Osteoarthritis Initiative, Skeletal Radiol. 48 (2019) 89–101, https://doi.org/10.1007/s00256-018-2995-4.

[6] J.H. Waarsing, S.M. Bierma-Zeinstra, H. Weinans, Distinct subtypes of knee osteoarthritis: data from the Osteoarthritis Initiative, Rheumatology (Oxford) 54 (2015) 1650–1658, https://doi.org/10.1093/rheumatology/kev100.

[7] A. Dell'Isola, M. Steultjens, Classification of patients with knee osteoarthritis in clinical phenotypes: data from the osteoarthritis initiative, PLoS One 13 (2018), e0191045, https://doi.org/10.1371/journal.pone.0191045.

[8] L.A. Deveza, A.E. Nelson, R.F. Loeser, Phenotypes of osteoarthritis: current state and future implications, Clin. Exp. Rheumatol. 37 (Suppl 120) (2019) 64–72.

[9] J. Favre, J.C. Erhart-Hledik, K. Blazek, B. Fasel, G.E. Gold, T.P. Andriacchi, Anatomically standardized maps reveal distinct patterns of cartilage thickness with increasing severity of medial compartment knee osteoarthritis, J. Orthop. Res. 35 (2017) 2442–2451, https://doi.org/10.1002/jor.23548.

[10] J. Favre, H. Babel, A. Cavinato, K. Blazek, B.M. Jolles, T.P. Andriacchi, Analyzing femorotibial cartilage thickness using anatomically standardized maps: reproducibility and reference data, J. Clin. Med. (2021) 10, https://doi.org/10.3390/jcm10030461.

[11] F.W. Roemer, S. Demehri, P. Omoumi, T.M. Link, R. Kijowski, S. Saarakkala, et al., State of the art: imaging of osteoarthritis-revisited 2020, Radiology 296 (2020) 5–21, https://doi.org/10.1148/radiol.2020192498.

[12] C. Huang, Z. Xu, Z. Shen, T. Luo, T. Li, D. Nissman, et al., DADP: dynamic abnormality detection and progression for longitudinal knee magnetic resonance images from the Osteoarthritis Initiative, Med. Image Anal. 77 (2022), 102343, https://doi.org/10.1016/j.media.2021.102343.

[13] Q. Feng, M.L. Jiang, J. Hannig, J.S. Marron, Angle-based joint and individual variation explained, J. Multivariate Anal. 166 (2018) 241–265, https://doi.org/10.1016/j.jmva.2018.03.008.

[14] G. Lester, The osteoarthritis initiative: a NIH public-private partnership, HSS J. 8 (2012) 62–63, https://doi.org/10.1007/s11420-011-9235-y.

[15] Q. Feng, J. Hannig, J.S. Marron, A note on automatic data transformation, Stat 5 (2016) 82–87, https://doi.org/10.1002/sta4.104.

[16] Z. Shen, X. Han, Z. Xu, M. Niethammer, Networks for joint affine and non-parametric image registration, IEEE Comput. Soc. Conf. Comput. Vis. Pattern Recogn. 2019 (2019) 4219–4228, https://doi.org/10.1109/cvpr.2019.00435.

[17] J.S. Marron, I.L. Dryden, Object Oriented Data Analysis, Chapman and Hall/CRC, 2021.

[18] E.F. Lock, K.A. Hoadley, J.S. Marron, A.B. Nobel, Joint and individual variation explained (jive) for integrated analysis of multiple data types, Ann. Appl. Stat. 7 (2013) 523–542, https://doi.org/10.1214/12-AOAS597.

[19] X. Yang, K.A. Hoadley, J. Hannig, J.S. Marron, Statistical Inference for Data Integration, 2021 arXiv:2109.12272.

[20] Y. Benjamini, Y. Hochberg, Controlling the false discovery rate: a practical and powerful approach to multiple testing, J. Roy. Statist. Soc. Series B-Methodol. 57 (1995) 289–300.

[21] A.E. Nelson, How feasible is the stratification of osteoarthritis phenotypes by means of artificial intelligence? Expert Rev. Precis. Med. Drug Dev. 6 (2021) 83–85, https://doi.org/10.1080/23808993.2021.1848424.

[22] A. Jamshidi, M. Leclercq, A. Labbe, J.P. Pelletier, F. Abram, A. Droit, et al., Identification of the most important features of knee osteoarthritis structural progressors using machine learning methods, Ther Adv Musculoskelet Dis 12 (2020), https://doi.org/10.1177/1759720X20933468, 1759720X20933468.

[23] A.A. Tolpadi, J.J. Lee, V. Pedoia, S. Majumdar, Deep learning predicts total knee replacement from magnetic resonance images, Sci. Rep. 10 (2020) 6371, https://doi.org/10.1038/s41598-020-63395-9.

[24] B. Guan, F. Liu, A.H. Mizaian, S. Demehri, A. Samsonov, A. Guermazi, et al., Deep learning approach to predict pain progression in knee osteoarthritis, Skeletal Radiol. (2021), https://doi.org/10.1007/s00256-021-03773-0.

[25] J.J. Lee, F. Liu, S. Majumdar, V. Pedoia, An ensemble clinical and MR-image deep learning model predicts 8-year knee pain trajectory: data from the osteoarthritis initiative, Osteoarthritis Imaging 1 (2021), 100003, https://doi.org/10.1016/j.ostima.2021.100003.

[26] A.G. Morales, J.J. Lee, F. Caliva, C. Iriondo, F. Liu, S. Majumdar, et al., Uncovering associations between data-driven learned qMRI biomarkers and chronic pain, Sci. Rep. 11 (2021) 21989, https://doi.org/10.1038/s41598-021-01111-x.

[27] J.B. Driban, M.S. Harkey, M.F. Barbe, R.J. Ward, J.W. MacKay, J.E. Davis, et al., Risk factors and the natural history of accelerated knee osteoarthritis: a narrative review, BMC Muscoskel. Disord. 21 (2020) 332, https://doi.org/10.1186/s12891-020-03367-2.

[28] L.A. Deveza, L. Melo, T.P. Yamato, K. Mills, V. Ravi, D.J. Hunter, Knee osteoarthritis phenotypes and their relevance for outcomes: a systematic review, Osteoarthritis Cartilage 25 (2017) 1926–1941, https://doi.org/10.1016/j.joca.2017.08.009.

[29] J.M. Jordan, C.G. Helmick, J.B. Renner, G. Luta, A.D. Dragomir, J. Woodard, et al., Prevalence of knee symptoms and radiographic and symptomatic knee osteoarthritis in african Americans and caucasians: the johnston county osteoarthritis project, J. Rheumatol. 34 (2007) 172–180.

[30] A.E. Nelson, D. Hu, A. Arbeeva, C. Alvarez, R.J. Cleveland, T.A. Schwartz, et al., The prevalence of knee symptoms, radiographic, and symptomatic osteoarthritis at four time points: the johnston county osteoarthritis project, 1999-2018, ACR Open Rheumatol. 3 (2021) 558–565, https://doi.org/10.1002/acr2.11295.

[31] A. Chang, M. Hochberg, J. Song, D. Dunlop, J.S. Chmiel, M. Nevitt, et al., Frequency of varus and valgus thrust and factors associated with thrust presence in persons with or at higher risk of developing knee osteoarthritis, Arthritis Rheum. 62 (2010) 1403–1411, https://doi.org/10.1002/art.27377.

[32] L. Braga, J.B. Renner, T.A. Schwartz, J. Woodard, C.G. Helmick, M.C. Hochberg, et al., Differences in radiographic features of knee osteoarthritis in African-Americans and Caucasians: the Johnston county osteoarthritis project, Osteoarthritis Cartilage 17 (2009) 1554–1561, https://doi.org/10.1016/j.joca.2009.07.011.

[33] N.J. Collins, E.H.G. Oei, J.L. de Kanter, B. Vicenzino, K.M. Crossley, Prevalence of radiographic and magnetic resonance imaging features of patellofemoral osteoarthritis in young and middle-aged adults with persistent patellofemoral pain, Arthritis Care Res. 71 (2019) 1068–1073, https://doi.org/10.1002/acr.23726.

[34] M. van Middelkoop, K.L. Bennell, M.J. Callaghan, N.J. Collins, P.G. Conaghan, K.M. Crossley, et al., International patellofemoral osteoarthritis consortium: consensus statement on the diagnosis, burden, outcome measures, prognosis, risk factors and treatment, Semin. Arthritis Rheum. 47 (2018) 666–675, https://doi.org/10.1016/j.semarthrit.2017.09.009.

[35] H.F. Hart, K.M. Crossley, M.A. Hunt, Gait patterns, symptoms, and function in patients with isolated tibiofemoral osteoarthritis and combined tibiofemoral and patellofemoral osteoarthritis, J. Orthop. Res. 36 (2018) 1666–1672, https://doi.org/10.1002/jor.23805.

[36] T.C. Liao, H. Jergas, R. Tibrewala, E. Bahroos, T.M. Link, S. Majumdar, et al., Longitudinal analysis of the contribution of 3D patella and trochlear bone shape on patellofemoral joint osteoarthritic features, J. Orthop. Res. 39 (2021) 506–515, https://doi.org/10.1002/jor.24836.